Temperature and Strain-Rate Dependence of Surface Dislocation Nucleation

Ting Zhu,[1,*] Ju Li,[2] Amit Samanta,[2] Austin Leach,[3] and Ken Gall[3,1]

[1]*Woodruff School of Mechanical Engineering, Georgia Institute of Technology, Atlanta, Georgia 30332, USA*
[2]*Department of Materials Science and Engineering, University of Pennsylvania, Philadelphia, Pennsylvania 19104, USA*
[3]*School of Materials Science and Engineering, Georgia Institute of Technology, Atlanta, Georgia 30332, USA*

(Received 2 July 2007; published 15 January 2008)

Dislocation nucleation is essential to the plastic deformation of small-volume crystalline solids. The free surface may act as an effective source of dislocations to initiate and sustain plastic flow, in conjunction with bulk sources. Here, we develop an atomistic modeling framework to address the probabilistic nature of surface dislocation nucleation. We show the activation volume associated with surface dislocation nucleation is characteristically in the range of $1–10b^3$, where b is the Burgers vector. Such small activation volume leads to sensitive temperature and strain-rate dependence of the nucleation stress, providing an upper bound to the size-strength relation in nanopillar compression experiments.

DOI: 10.1103/PhysRevLett.100.025502 PACS numbers: 62.20.−x, 61.72.Lk, 82.20.Pm

Small-volume materials with large surface areas have increasingly become the basic building blocks of modern technology. The mechanical properties of such surface-confined materials are drastically different from their macroscale counterparts. Recent mechanical testing of small-volume metals have measured unusually high strength, at levels of a significant fraction of their ideal strength. For example, uniaxial compression of single-crystal Au pillars with diameter 300 nm [1–3] gave flow strengths ~800 MPa. In comparison, the predicted ideal bulk shear strength of Au is only 850 MPa to 1.4 GPa, depending on the mode of loading [4]. Since surface is itself a defect, with significantly miscoordinated atoms compared to the perfect crystal [5], it is natural to ask to what degree the strength of a small-volume material reflects surface properties and surface-mediated processes [6–8], particularly when the sample size is in the range of tens of nm [9].

Dislocation nucleation is expected to be an important factor in the deformation of small-volume materials at low temperature [1,10,11]. In macroscale materials, the density of dislocations increases rapidly once deformation starts, due to double cross slip and other Frank-Read [12] type multiplication processes. In contrast, dislocation multiplication in small-volume samples must contend with dislocation loss from free surfaces, which could lead to dislocation starvation in the bulk. It is also possible that in small-volume materials, the initial configuration does not contain a single dislocation in it [9]. Under these dislocation-starved scenarios, dislocation nucleation from the surface potentially plays a critical role in controlling plastic deformation.

Molecular dynamics (MD) simulations have often been used to probe dislocation nucleation in the bulk crystal and from the surface [13,14]. While MD simulations have revealed rich atomic-scale details of dislocation nucleation processes, they provide less quantitative information regarding plasticity in normal laboratory experiments because of the extreme strain rate ($\dot{\epsilon} \sim 10^7–10^9/\mathrm{s}$) applied. A natural question to ask is: to what degree does the MD result reflect real deformation physics in laboratory experiments where the strain rate is typically $<1/\mathrm{s}$. To understand the nature of surface nucleation, and to enable quantitative correlations between MD and experimental results, here we take a related but different approach that combines transition state theory and detailed atomistic energy landscape [15]. Such approach allows us to predict the nucleation stress over a large range of temperatures and strain rates, and reveal its statistical nature [16,17] without the limitation of excessive strain rates.

Surface dislocation sources can be characterized by two quantitative measures: athermal strength and activation parameters. The former measures the elastic limit of the surface, at which a dislocation nucleates instantaneously without the aid of thermal fluctuations. The activation parameters, including the activation energy and activation volume, characterize the probabilistic nature of dislocation nucleation by thermal fluctuation when the applied load is below the athermal limit. Specifically, at a given temperature T and stress σ, the nucleation rate is

$$\nu = N\nu_0 \exp\left(-\frac{Q(\sigma, T)}{k_B T}\right). \tag{1}$$

Here, ν_0 is the attempt frequency, N is the number of equivalent surface nucleation sites, $k_B T$ is the thermal energy, and Q is the activation free energy [11] whose magnitude is controlled by the local stress σ. The activation volume Ω, defined as the derivative of activation free energy with stress, i.e., $\Omega(\sigma, T) \equiv -\partial Q/\partial\sigma|_T \approx k_B T \partial \ln(\nu)/\partial\sigma$, measures the sensitivity of nucleation rate to stress. While the athermal surface strength has received significant attention in recent years [5,6], the activation parameters of surface dislocation source have not been quantitatively studied using the atomistic approach.

Equation (1) gives the nucleation rate when the system is under constant stress. But in experiments, constant strain rate is more commonly used. Consider a dislocation-free nanowire under constant *elastic* strain rate $\dot{\epsilon}$, such that the

stress σ and time t are directly related by $\sigma = E\dot{\epsilon}t$, where E denotes the apparent Young's modulus of the wire. The probabilistic nature of a thermally activated nucleation process dictates that the nucleation stress is a distribution rather than a constant value when many repeated tests are performed. One can define the (most probable) nucleation stress as the load when the dislocation forms most frequently. An implicit expression [16,17] can be derived for the nucleation stress when the wire is under constant *temperature* and *strain rate* [18],

$$\frac{Q(\sigma, T)}{k_B T} = \ln\frac{k_B T N \nu_0}{E\dot{\epsilon}\Omega(\sigma, T)}. \quad (2)$$

In a first approximation of the temperature effect on the activation free energy $Q(\sigma, T)$ [19], we take $Q(\sigma, T) = (1 - T/T_m)Q_0(\sigma)$, where T_m is the surface disordering temperature, and $Q_0(\sigma)$ is the activation energy on the zero-T potential energy surface (PES). It follows that the activation volume $\Omega(\sigma, T) = (1 - T/T_m)\Omega_0(\sigma)$, where $\Omega_0 \equiv -dQ_0/d\sigma$. The prediction of nucleation stress is then reduced to the problem of finding the minimum energy path (MEP) [20] of nucleation on the zero-T PES; namely, $Q_0(\sigma)$ can be calculated as the energy difference between the saddle point and initial equilibrium state on the MEP, and ν_0 is vibrational frequency of the normal mode in the MEP reaction coordinate direction at the initial equilibrium state. One can determine the MEP by using, for example, the free-end nudged elastic band (FENEB) method [15], developed recently to efficiently explore strongly driven reactions.

To apply the above atomistically-based, nonlinear theory to predict surface dislocation nucleation, we have studied a model system of a Cu nanowire deformed under uniaxial compression [18]. The wire is initially a perfect crystal with a [001] axis. It has a square cross section and {100} side faces, see Fig. 1(a). We study representative unit processes of the nucleation of a Shockley partial dislocation on one of the $\{111\}\langle 11\bar{2}\rangle$ slip systems for which the resolved shear stress is maximized. Parenthetically, there are generally three surface nucleation scenarios: (A) a single leading partial dislocation, (B) a full dislocation, with complementary leading and trailing partials, and (C) deformation twinning. The present study focuses on a leading partial dislocation because even in the cases of (B) and (C), nucleation of the first leading partial is usually the most difficult, rate-limiting step [21]. Two representative (competing) nucleation sites are examined: the middle of side surface, which is atomically flat, and the 90° sharp corner, which is an extreme case of heterogeneous surface nucleation. When the wire is under a prescribed compressive stress, e.g., 3.3 GPa (the corresponding compressive strain is 0.085), Fig. 1(b) and 1(c) show, respectively, the saddle-point atomic configurations of nucleation from the side surface and the corner, both of which are identified by the FENEB calculation. The area enclosed by the loop corresponds to the activation area that the dislocation line has swept out between the stable (perfect wire without dislocations) and unstable (saddle-point) equilibrium states. Physically, the size of the activation area is proportional to the activation volume, which is to be quantitatively evaluated. We calculate the activation energy Q_0, and obtain $Q_0 = 0.64$ eV for nucleation from the side surface and $Q_0 = 0.1$ eV for corner nucleation. Assuming the same attempt frequency for the two processes, Eq. (1) dictates that the nucleation from corners dominates over competing surface sources such as atomically smooth surface. The favored mode of corner nucleation has been confirmed by our direct MD simulations. We hereafter focus on the corner nucleation, and study the temperature and strain rate dependence of the nucleation stress.

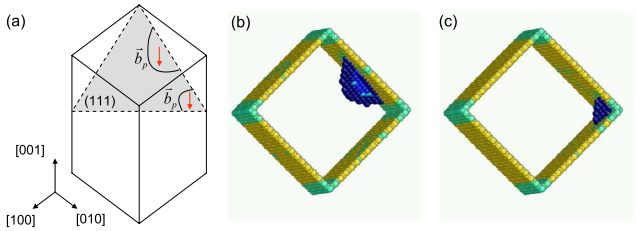

FIG. 1 (color online). Reaction pathway modeling of dislocation nucleation from a Cu nanowire under uniaxial compression. (a) Schematics of a [001] wire showing the Shockley partial dislocation loop (the Burgers vector $\vec{b}_p = \langle 11\bar{2}\rangle/6$); (b) Saddle-point configuration of an embryonic dislocation loop emanating from the atomically smooth side surface; (c) Saddle-point structure of the loop nucleation from an atomically sharp corner. Atoms are colored by the breaking of local inversion symmetry.

Next, consider the corner dislocation nucleation in a nanowire under constant strain rate. Prediction of nucleation stress based on Eq. (2) requires atomistic input of stress dependent activation energy and activation volume. In Fig. 2(a), we show with circles the calculated activation energies of corner nucleation at different stresses; the solid line is a fitting curve by taking the functional form $Q_0(\sigma) = A(1 - \sigma/\sigma_{\text{ath}})^{\alpha}$, we obtain $A = 4.8$ eV, $\sigma_{\text{ath}} = 5.2$ GPa, and $\alpha = 4.1$. In Fig. 2(b), we show the activation volume as a function of stress, which is calculated by

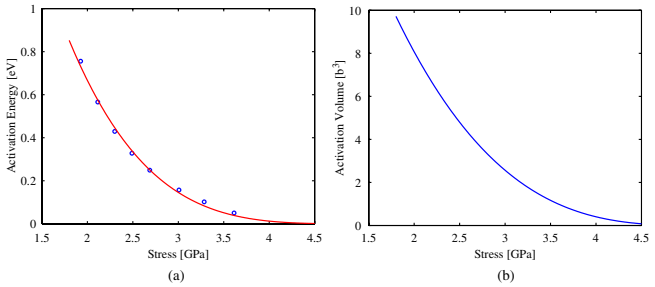

FIG. 2 (color online). Stress-dependent activation parameters for dislocation nucleation from the corner of a Cu nanowire: (a) Circles show the calculated activation energy as a function of stress and the solid line is the fitting curve. (b) The activation volume as a function of stress.

taking the derivative of $Q_0(\sigma)$ with respect to σ. The magnitude of activation volume is found to be rather small. For example, when $Q_0 \approx 0.6$ eV, a barrier giving a nucleation rate comparable to typical laboratory experiments (seconds to hours time scale) at room temperature, the corresponding activation volume Ω_0 is about $5b^3$. Moreover, our calculations show that for dislocation nucleation from other types of surface sources, e.g., atomically smooth surface [see Fig. 1(b)], the associated activation volumes are similarly small, about $10b^3$. We also change the (100) surface to (111) surface, as well as create surface steps on the (111) surface with and without kinks. We find that when $Q_0(\sigma) = 0.6$ eV, the corresponding activation volumes are about $2b^3$. Altogether, these data show surface dislocation nucleation has activation volumes in the range of 1–$10b^3$. The physical significance of such characteristic activation volume will be demonstrated next on the temperature and strain-rate sensitivity of nucleation stress.

For corner nucleation, Fig. 3 shows the nucleation stresses (solid lines) predicted by numerically solving Eq. (2) with $Q_0(\sigma)$ and $\Omega_0(\sigma)$ as an input [18]. Here, the nucleation stress is plotted as a function of temperature at two characteristic strain rates, $\dot{\epsilon} = 10^{-3}/\mathrm{s}$ and $\dot{\epsilon} = 10^{8}/\mathrm{s}$, which are typical of laboratory experiments and MD simulations, respectively. To verify theoretical predictions, we have performed direct MD simulations under constant strain rate (about $10^8/\mathrm{s}$) and isothermal conditions. Figure 3 also shows the nucleation stresses (circles) collected from MDs; the scattering of nucleation stresses from MDs is attributed to the effect of thermal uncertainty. Evidently, transition-state-theoretic predictions agree with direct numerical experiments at high strain rates.

The nucleation stresses in Fig. 3 show significant temperature sensitivity. Particularly, we note that under a low strain rate of $\dot{\epsilon} = 10^{-3}/\mathrm{s}$, the nucleation stress drops by more than 70% as T increases from nearly zero to room temperature. This result clearly underscores the importance of the temperature effect in correlating the zero-T calculations (e.g., ideal surface strength) [5,6] with room-temperature experimental measurements (e.g., compressive strength of nanowires or nanopillars).

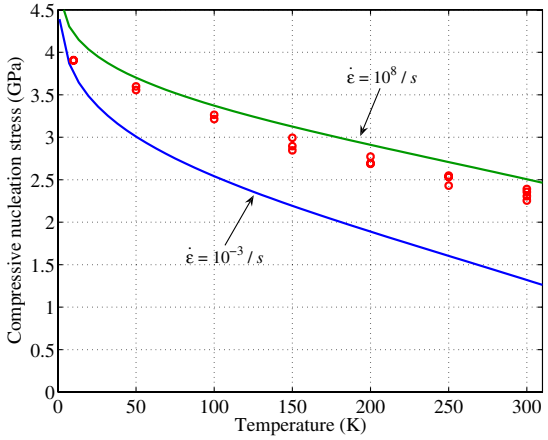

FIG. 3 (color online). Nucleation stress as a function of temperature and strain rate from predictions (solid lines) and direct MD simulations (circles).

The sensitive temperature dependence of nucleation stress arises because of the characteristically small activation volume associated with surface sources. To render this point physically transparent, let us consider a simple case where the activation energy depends linearly on stress. Suppose one knows the activation volume $\hat{\Omega}$ at a given stress, denoted as $\hat{\sigma}$, the activation energy Q near $\hat{\sigma}$ can be approximated by a linear relation $Q(\sigma) = Q(\hat{\sigma}) - \hat{\Omega}(\sigma - \hat{\sigma})$, or equivalently $Q(\sigma) = Q^* - \sigma\hat{\Omega}$, where $Q^* \equiv Q(\hat{\sigma}) + \hat{\sigma}\,\hat{\Omega}$ and it corresponds to the nucleation barrier in the absence of applied stress within the linear approximation of stress-dependent activation energy. The nucleation stress given by Eq. (2) is then

$$\sigma = \frac{Q^*}{\hat{\Omega}} - \frac{k_B T}{\hat{\Omega}} \ln \frac{k_B T N \nu_0}{E\dot{\epsilon}\,\hat{\Omega}}. \tag{3}$$

Here, the first term $Q^*/\hat{\Omega}$ is the athermal nucleation stress causing instantaneous dislocation nucleation in the linearized model of stress-dependent activation energy. The prefactor of the second term $k_B T/\hat{\Omega}$ has a stress unit, and it sets the scale of nucleation stress reduction due to thermal fluctuation. In the logarithmic function, $k_B T N \nu_0$ is the rate of energy exchange of the candidate nucleation sites with the thermal bath, and $E\dot{\epsilon}\,\hat{\Omega}$ is the rate of activation energy reduction by the mechanical work. The ratio between the two terms determines the competition of thermal and mechanical effects in mediating the nucleation stress reduction ($\propto k_B T/\hat{\Omega}$) due to thermal fluctuations.

Equation (3) explicitly shows the functional dependence of nucleation stress on temperature and strain rate; namely, σ scales, respectively, with $T \ln T$ and $\ln\dot{\epsilon}$. Since T premultiplies the logarithm, the nucleation stress should be most sensitive to temperature, particularly when the activation volume $\hat{\Omega}$ is small. Recall that in Fig. 2, we show within a range of barrier from 0.1 to 0.6 eV that controls the rate processes in Fig. 3, the activation volume varies, but it remains in a characteristic range of a few b^3. Such small activation volume causes the sensitive temperature dependence of nucleation stress, as shown in Fig. 3. It is important to note that the activation volume for a typical bulk dislocation source, such as the Frank-Read source, is between 100–$1000b^3$, leading to the commonly observed rate-insensitive plastic yield in large crystals at room temperature. This large difference in activation volume between surface and bulk dislocation processes suggests that activation volume can be taken as a kinetic signature of deformation mechanism [22]. Additionally, while the strain rate $\dot{\epsilon}$ is inside the logarithm in Eq. (3), its effect could be significant on the predicted nucleation stress. For example, if one needs to quantitatively correlate atomistic

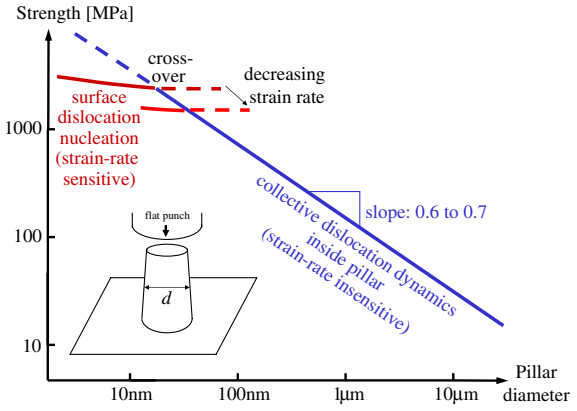

FIG. 4 (color online). Illustration of surface effect on the rate-controlling process: size dependence of yield strength in single-crystal wires or pillars under compression. A power-law scaling was measured in micron-sized pillars [23], where the rate insensitive plastic yield is governed by dislocation dynamics inside the pillar. In very small pillars, surface dislocation nucleation is expected to dominate, giving a logarithmic dependence of yield stress to the pillar size and providing an upper bound to the size-strength relation in nanopillar compression experiments; this upper bound is strain-rate sensitive because of the small activation volume.

calculation results with laboratory experiments, the influence of strain rate could not be ignored, as shown in Fig. 3.

Equation (3) also reveals a size effect on the nucleation stress [16,17] because a change in the wire geometry directly affects the number of equivalent surface nucleation sites N. Since N is in the logarithmic function of Eq. (3), the size effect arising from surface nucleation is expected to be weak, compared to that in micropillars showing a power-law scaling with an exponent in the range from -0.6 to -0.7 [3,23]. The latter scaling behavior likely arises from collective dislocation dynamics inside the pillar [23] involving dislocation interactions and multiplications, when the pillar volume is large enough to sustain such a population. Since surface dislocation nucleation likely dominates plastic yielding in the nanoscale samples due to dislocation source starvation in the bulk, one thus expects a transition in the scaling behavior of yield stress on the sample size in an approximate range of tens of nanometers, as illustrated by Fig. 4. Recent experiments on the nanoscale samples show hints of such transition [1–3], but more detailed experimental and modeling studies are needed. Finally, we note that a change in the wire geometry will also affect the activation energy Q_0 and the activation volume Ω_0 due to the long range elastic interaction associated with the image effects of free surface of the sample, as well as the effect of internal stress of other corners. To evaluate their quantitative influences, we have studied a wire with the side length doubled. When Q_0 varies between 0.24–0.52 eV, the averaged Ω_0 is about $4b^3$, consistent with the previous results that the activation volume of surface dislocation nucleation is in the range of $1–10b^3$.

In conclusion, the present work addresses the surface dislocation nucleation aspect of small scale plasticity. We find surface sources have a unique kinetic signature: a small activation volume leading to increased strain-rate and temperature sensitivities of flow stress. A transition in the rate-controlling flow mechanism is predicted from collective dislocation dynamics to single dislocation nucleation for small-volume materials with length scale of tens of nanometers.

T. Z. is supported by NSF Grant No. CMMI-0653769. J. L. and A. S. are supported by NSF Grant No. DMR-0502711, ONR Grant No. N00014-05-1-0504, AFOSR.

*ting.zhu@me.gatech.edu

[1] J. R. Greer and W. D. Nix, Phys. Rev. B **73**, 245410 (2006).
[2] C. A. Volkert and E. T. Lilleodden, Philos. Mag. **86**, 5567 (2006).
[3] C. A. Volkert, E. T. Lilleodden, D. Kramer, and J. Weissmuller, Appl. Phys. Lett. **89**, 061920 (2006).
[4] S. Ogata *et al.*, Phys. Rev. B **70**, 104104 (2004).
[5] S. V. Dmitriev *et al.*, Acta Mater. **53**, 1215 (2005).
[6] S. Brochard, P. Beauchamp, and J. Grilhe, Philos. Mag. A **80**, 503 (2000).
[7] J. A. Zimmerman *et al.*, Phys. Rev. Lett. **87**, 165507 (2001).
[8] C. Li and G. Xu, Philos. Mag. **86**, 2957 (2006).
[9] K. Sieradzki *et al.*, Acta Mater. **54**, 4533 (2006).
[10] M. J. Cordill *et al.*, Acta Mater. **54**, 4515 (2006).
[11] J. Li, MRS Bull. **32**, 151 (2007).
[12] F. C. Frank and W. T. Read, Phys. Rev. **79**, 722 (1950).
[13] J. K. Diao, K. Gall, and M. L. Dunn, Nano Lett. **4**, 1863 (2004).
[14] E. Rabkin, H.-S. Nam, and D. J. Srolovitz, Acta Mater. **55**, 2085 (2007).
[15] T. Zhu *et al.*, Proc. Natl. Acad. Sci. U.S.A. **104**, 3031 (2007).
[16] J. K. Mason, A. C. Lund, and C. A. Schuh, Phys. Rev. B **73**, 054102 (2006).
[17] A. H. W. Ngan, L. Zuo, and P. C. Wo, Proc. R. Soc. A **462**, 1661 (2006).
[18] See EPAPS Document No. E-PRLTAO-100-026802 for supplementary material. For more information on EPAPS, see http://www.aip.org/pubservs/epaps.html.
[19] N. F. Mott, Proc. Phys. Soc. London **60**, 391 (1948).
[20] G. Henkelman, B. P. Uberuaga, and H. Jonsson, J. Chem. Phys. **113**, 9901 (2000).
[21] S. Ogata, J. Li, and S. Yip, Phys. Rev. B **71**, 224102 (2005).
[22] R. J. Asaro and S. Suresh, Acta Mater. **53**, 3369 (2005).
[23] D. M. Dimiduk, M. D. Uchic, and T. A. Parthasarathy, Acta Mater. **53**, 4065 (2005).

Temperature and Strain-Rate Dependence of Surface Dislocation Nucleation

Ting Zhu[1], Ju Li[2], Amit Samanta[2], Austin Leach[3] and Ken Gall[3,1]

[1] *Woodruff School of Mechanical Engineering, Georgia Institute of Technology, Atlanta, Georgia 30332, USA*

[2] *Department of Materials Science and Engineering, University of Pennsylvania, Philadelphia, Pennsylvania 19104, USA and*

[3] *School of Materials Science and Engineering, Georgia Institute of Technology, Atlanta, Georgia 30332, USA*

(Dated: November 21, 2007)

Supplementary information

Model and Method

The wire has an initial axial length $l_0 = 7.23$nm and side length $a_0 = 5.42$nm. The total number of atoms within the system is $18,000$. The atomic interactions are modeled using the embedded atom method (EAM) potential of Mishin et al.[1]. Although most experiments were performed on Au[2–4], EAM potentials for Au are unsatisfactory in reproducing its elastic and surface properties. The EAM Cu potential employed in this work has been extensively validated by comparing with first-principles calculations[5]. Periodic boundary condition is imposed along the axial direction and the side surfaces are free. We apply the uniaxial load by varying the length l of the simulation cell in the axial direction and allow all the atoms to freely relax. The axial stress is defined by $\sigma \equiv lF/l_0a_0^2$, where F denotes the axial force; here we have assumed the volume change is small, which has been verified by direct calculations. The axial strain $\epsilon \equiv \Delta l/l_0$, where Δl denotes the change in length of the wire.

Under a given axial strain (stress), we employ the climbing image nudged elastic band (CINEB) method[6] to determine the minimum energy path (MEP) of dislocation nucleation by thermal activation. The activation energy Q_0 is the energy difference between the saddle-point and initial states on the MEP. In a CINEB calculation, two end-states are first determined, then a discrete elastic band consisting of a finite number of replicas (images) of the system is constructed by linear interpolation to connect the two end-states. With appropriate relaxation, the band converges to the MEP.

In CINEB calculations, we choose an initial state where a perfect nanowire (under a prescribed strain) is fully relaxed, and a final state where an embryonic dislocation loop has formed in the wire (at the same axial strain as the initial state), but before the loop has propagated away. To create this final state, the embryonic dislocation loop can be generated by direct molecular dynamics simulation, which is time consuming because of the rare-event nature of thermally activated processes. Alternatively, a scheme of steered nucleation can be programmed that involves consecutive operations of cut, shift, and constrained relaxation.

To obtain a fully relaxed and stable elastic band, we have improved the original CINEB method by allowing a free end state, while keeping its energy unchanged; such scheme is called free-end nudged elastic band (FENEB) method[7]. In this way, one can keep the end state close to the saddle-point/initial states in terms of the difference in energy or the

hyperspace distance. In our calculations the energy of the final state is fixed at 0.1eV below the initial state. As a result, the number of replicas along the band can be significantly reduced while retaining a reasonable density of replicas near the saddle point, e.g., eight replicas are sufficient to obtain a converged saddle-point state that we have double-checked using the dimer method[8]. The FENEB calculation is considered converged when the force on each replica perpendicular to the path is less than 0.002 eV/A.

One can also determine the physical attempt frequency ν_0 from NEB calculations. For monatomic systems, ν_0 can be computed as $\nu_0 = \frac{1}{2\pi}\sqrt{\frac{C}{m}}$, where m is the mass of one atom, and $C = \frac{d^2V(\mathbf{x}^{3N}_{\text{MEP}}(s))}{ds^2}|_{s=0}$ is the initial energy curvature along the minimum energy path, where $s \equiv \int_{\mathbf{x}^{3N}_{\text{initial}}} \sqrt{d\mathbf{x}^{3N}_{\text{MEP}} \cdot d\mathbf{x}^{3N}_{\text{MEP}}}$ is the hyperspace arc length labeling this curve.

Fig. 3 (in the text) shows the nucleation stresses (solid lines) predicted by numerically solving Eq. (2) (in the text) with $Q_0(\sigma)$ and $\Omega_0(\sigma)$ as an input. The relevant parameters are determined as follows. The attempt frequency from FENEB calculation is $\nu_0 = 3.14\times10^{11}$/s. The number of equivalent nucleation sites is $N = 160$. This is because there are a total of 80 atoms at the four corners of the wire, and there are two equivalent slip systems at each atomic site, such that $N = 160$. The surface disordering temperature is taken as $T_m = 700$K, about one-half of the bulk melting temperature. Here, T_m is approximate. The determination of precise T_m is beyond the scope of this paper. To achieve a better prediction, T_m can be taken as a *single* adjustable parameter in this modeling framework, and it can be calibrated by experiments.

The mean nucleation stress given in Eq. (2) in the text can be derived as follows. Define f as the survival probability of an initially elastic wire,

$$\frac{df(t)}{dt} = -\nu f(t). \tag{1}$$

where ν is the nulceation rate given by Eq. (1) in the text. Because the load is applied via constant strain rate $\dot{\epsilon}$, the stress σ and time t are directly related by $\sigma = E\dot{\epsilon}t$, so

$$\frac{df(\sigma)}{d\sigma} = -\frac{\nu(\sigma)}{E\dot{\epsilon}} f(\sigma) \tag{2}$$

As σ increases, $f(\sigma)$ decreases and $\nu(\sigma)$ increases, giving rise to a maximum of $df(\sigma)/d\sigma$. The most probable nucleation stress is defined by the peak of $df(\sigma)/d\sigma$,

$$\frac{d^2 f}{d\sigma^2} = 0. \tag{3}$$

Substitution of Eq. (1) (in the text) and Eq. (2) into Eq. (3) yields Eq. (2) (in the text).

---

[1] Y. Mishin, M. J. Mehl, D. A. Papaconstantopoulos, A. F. Voter, and J. D. Kress, Phys. Rev. B **63**, 224106 (2001).

[2] J. R. Greer and W. D. Nix, Phys. Rev. B **73**, 245410 (2006).

[3] C. A. Volkert and E. T. Lilleodden, Philos. Mag. **86**, 5567 (2006).

[4] C. A. Volkert, E. T. Lilleodden, D. Kramer, and J. Weissmuller, Appl. Phys. Lett. **89**, 061920 (2006).

[5] T. Zhu, J. Li, K. J. Van Vliet, S. Ogata, S. Yip, and S. Suresh, J. Mech. Phys. Solids **52**, 691 (2004).

[6] G. Henkelman, B. P. Uberuaga, and H. Jonsson, J. Chem. Phys. **113**, 9901 (2000).

[7] T. Zhu et al., Proc. Natl. Acad. Sci. USA **104**, 3031 (2007).

[8] G. Henkelman and H. Jonsson, J. Chem. Phys. **111**, 7010 (1999).